

Au-Ni synergy for enhanced electrochemical oxidation of ethanol over Au/Ni foam electrode

Xing Tan,^a Ruixing Du,^a Qitong Zhong,^a Longfei Liao,^b Huanhao Chen,^a Zhenchen Tang,^a Dafeng Yan,^c Shiming Chen,^d Feng Zeng^{a,*}

^a State Key Laboratory of Materials-Oriented Chemical Engineering, College of Chemical Engineering, Nanjing Tech University, Nanjing 211816, Jiangsu, China

^b School of Materials Science and Engineering, Harbin Institute of Technology (Shenzhen), Shenzhen 518055, Guangdong, China

^c College of Chemistry and Chemical Engineering, Hubei University, Wuhan 430062, China

^d School of Intelligent Medicine, China Medical University, Shenyang 110122, Liaoning, China

* Email: zeng@njtech.edu.cn

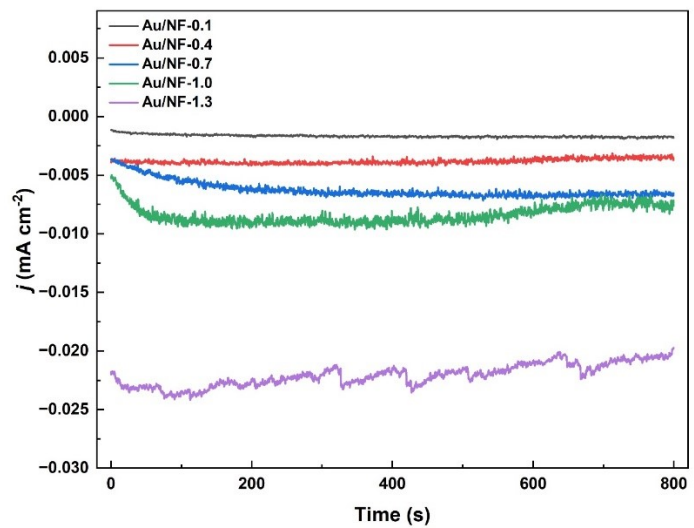


Figure S1. Electrodeposition current of Au/NF electrodes.

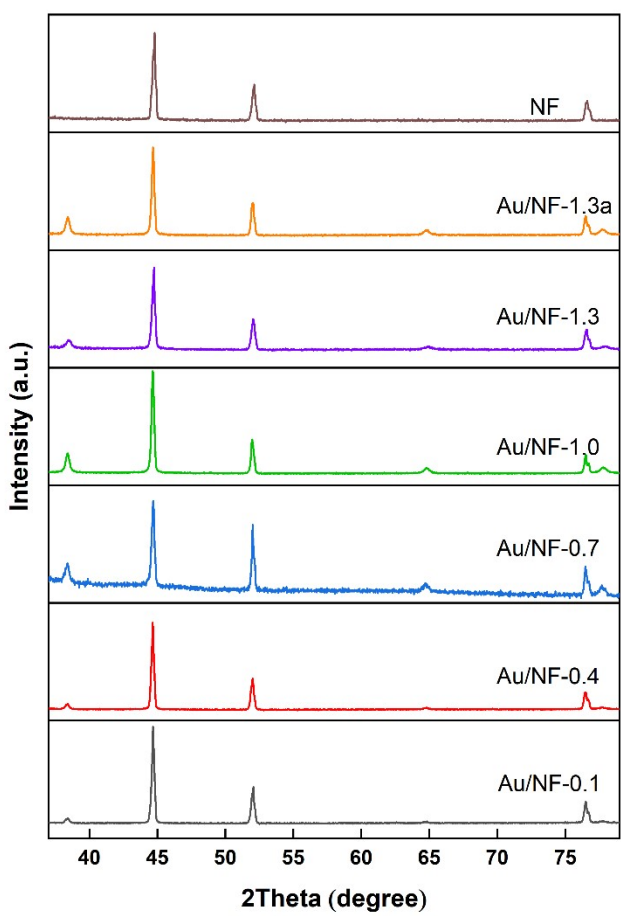


Figure S2. XRD of Au/NF catalyst and nickel foam.

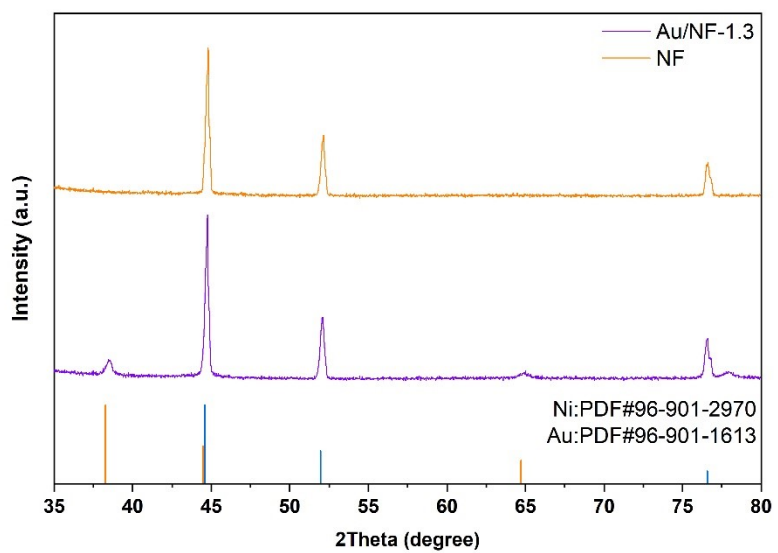


Figure S3. XRD of Au/NF-1.3 and NF catalyst and nickel foam.

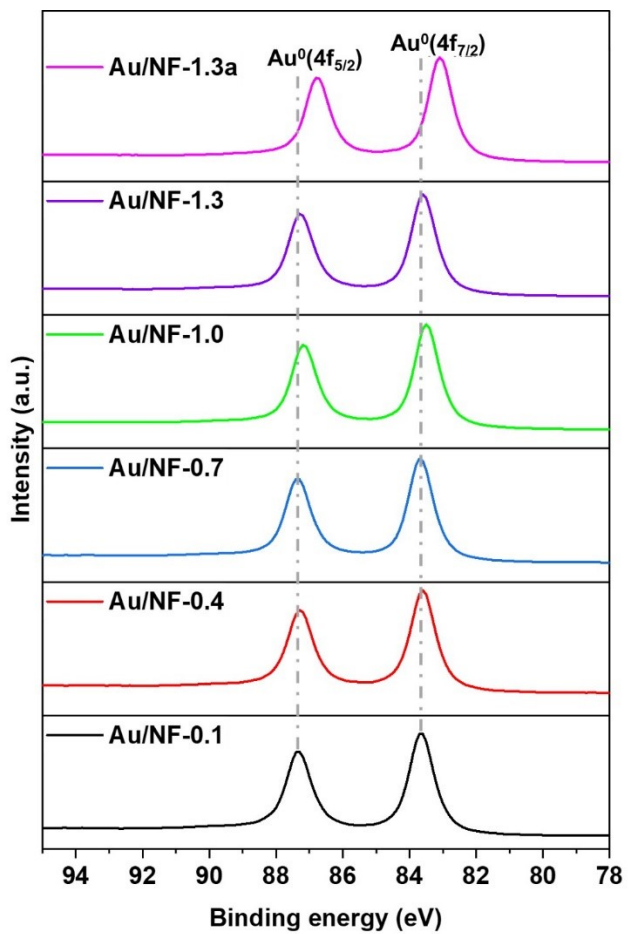


Figure S4. Au 4f XPS spectrum of Au/NF electrodes.

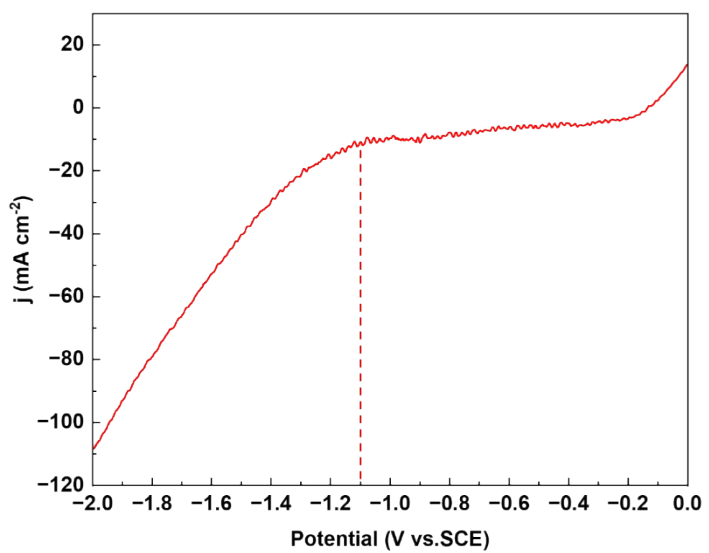


Figure S5. The linear sweep voltammetry (LSV) plot over nickel foam in a 0.5 M Na_2SO_4 and 0.5 mM HAuCl_4 solution with a scan rate of 20mV s^{-1} .

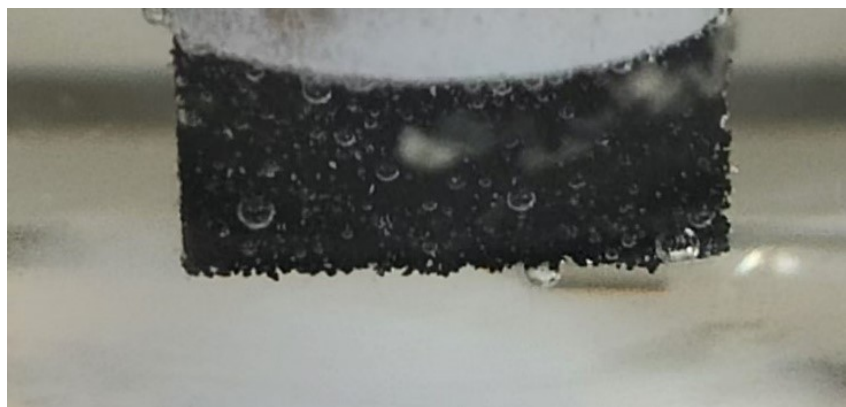


Figure S6. Gas bubbles observed on the surface of the Au/NF-1.3 electrode during the electrodeposition process.

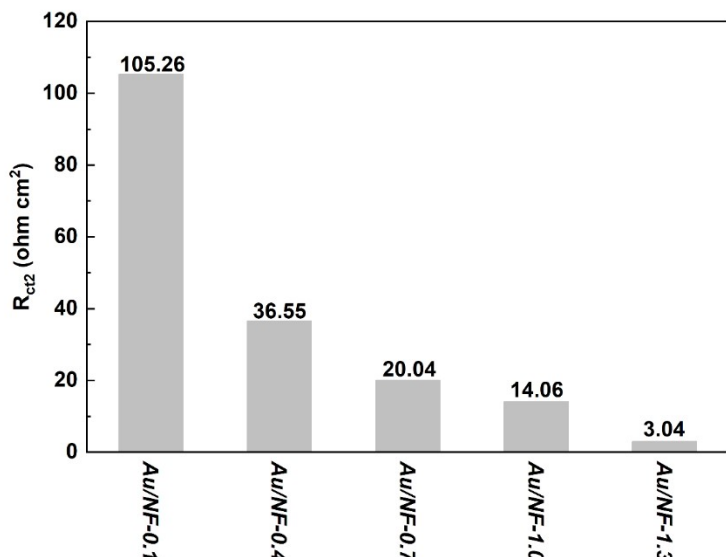


Figure S7. R_{ct2} of Au/NF electrodes during EOR.

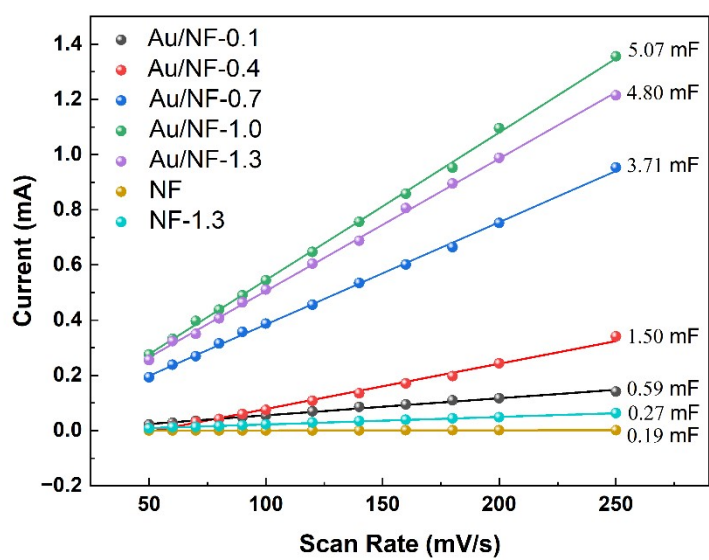


Figure S8. Anodic charging current densities measured at the potential 0.45 V vs. RHE plotted as a function of scan rate. The slope of the linear fit gives the double layer capacitance.

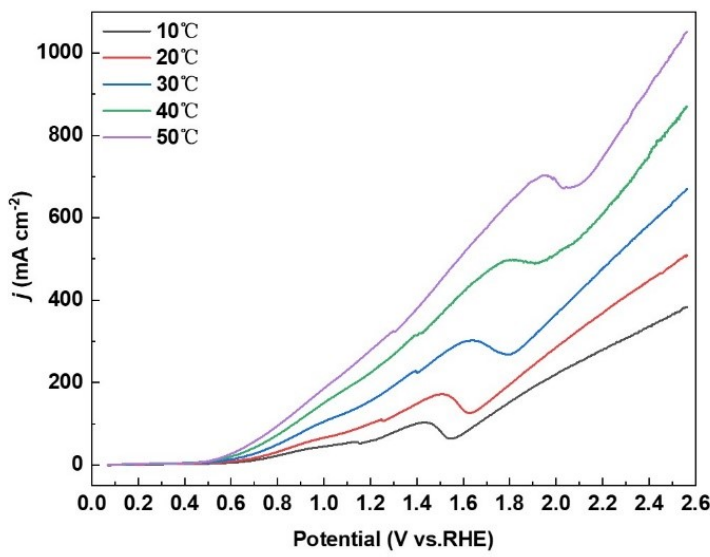


Figure S9. LSV plots (50 mV s^{-1}) obtained over Au/NF-1.3 electrode at various temperature in 1 M KOH and 1 M ethanol.

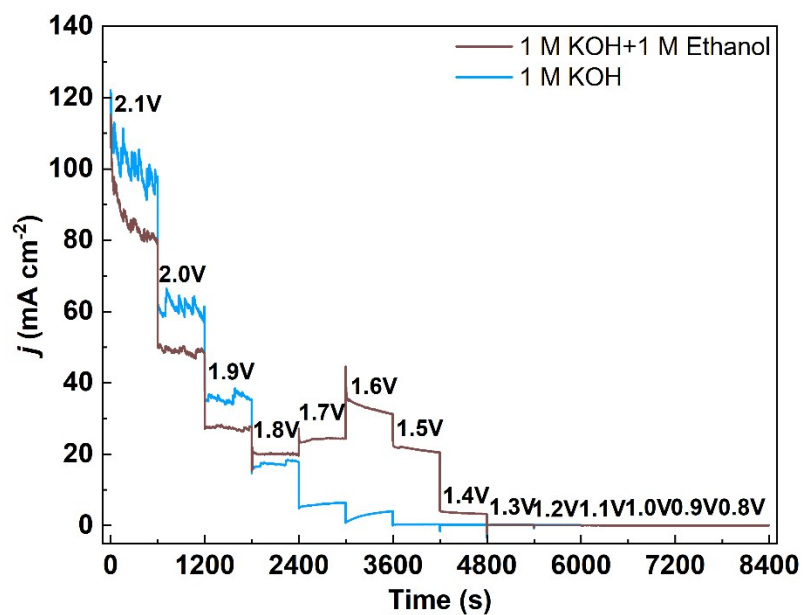


Figure S10. The stepped potential CA plots Au free NF-1.3 in electrolytes with and without ethanol.

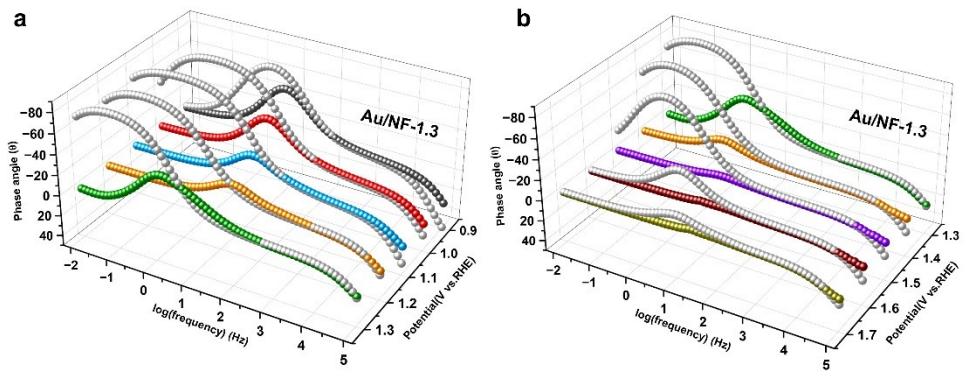


Figure S11. Bode plots of Au/NF-1.3 catalysis over the (c) potential range from 0.9 to 1.3 V and (d) potential range from 1.3 to 1.7 V in 1 M KOH (color dot) with 1 M ethanol or

1M

KOH

(gray)

spot

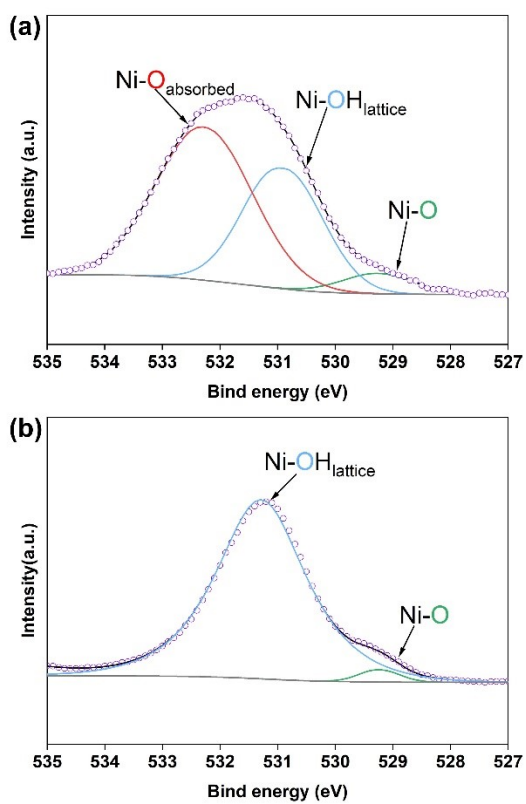


Figure S12. XPS O 1s spectra of (a) Au/NF-1.3 and (b) NF-1.3.

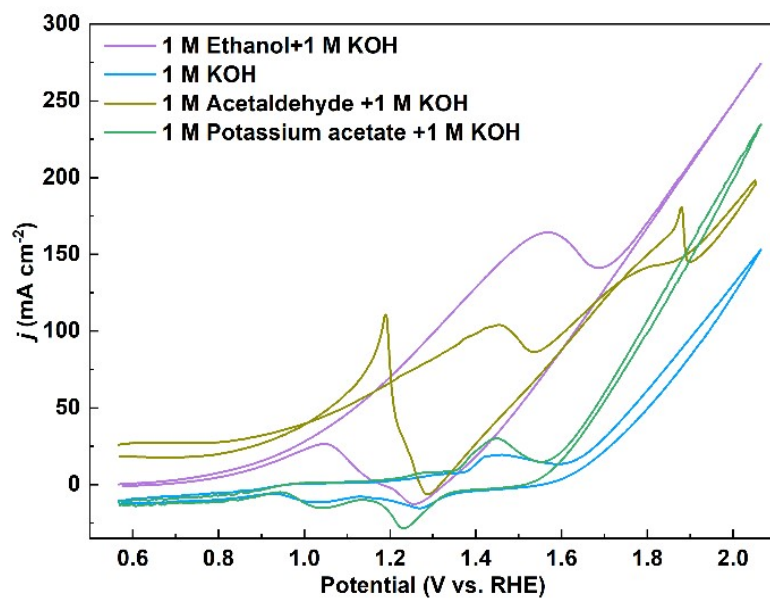


Figure S13. CV curves of Au/NF-1.3 in 1 M KOH, 1 M KOH with 1 M ethanol, 1 M KOH with 1 M acetaldehyde, 1 M KOH with 1 M potassium acetate, scanned at 50 mV s⁻¹.

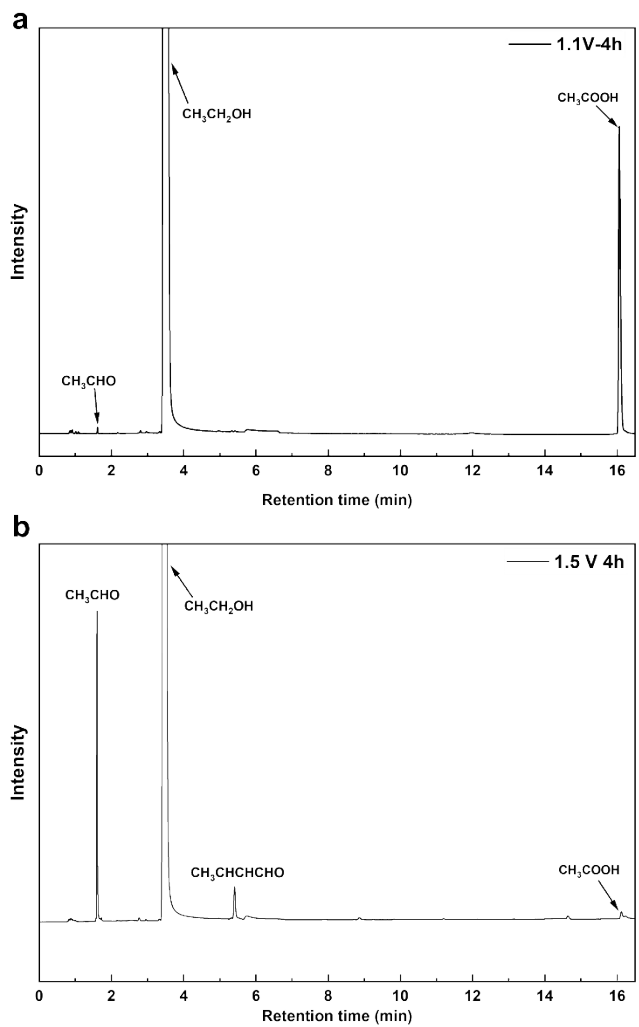


Figure S14. The gas chromatogram of the electrolyte after 4 hours of reaction using the Au/NF-1.3 catalyst in 1 M ethanol and 1 M KOH solutions at (a) 1.1 V vs. RHE and (b) 1.5 V vs. RHE.

Table S1. EOR performance of catalysts in this work in comparison with state-of-the-art catalysts.

Catalyst	Electrolyte	Peak potential (V _{RHE})	Peak current density (mA cm ⁻²)	ECSA (cm ²)/(cm ² g ⁻¹)	Ref.
NF	1 M KOH +1 M EtOH	1.58	29.7	0.51 / 25.28	This work
Au/NF-1.3		1.57	164	12.44 / 595.21	
NF-1.3		1.68	88.7	0.70 / 35.49	
Au/NF-0.1		1.27	24.6	1.54 / 76.62	
Au/NF-0.4		1.31	52.5	3.89 / 189.76	
Au/NF-0.7		1.36	65.2	9.66 / 464.42	
Au/NF-1.0		1.42	96.7	13.13 / 625.24	
Au/MnO₂/NF	0.5 M KOH + 0.5 M EtOH	1.60	64.0	-	[1]
NiF/AuNPs	0.5 M NaOH + 1 M EtOH	1.21	6.4	-	[2]
Au@PdAu_{1.8L}	1 M KOH +1 M EtOH	0.91	32.7	-	[3]
Au@AuPd	0.5 M KOH + 1 M EtOH	0.93	24.8	-	[4]
Au@Pd	1 M NaOH + 1 M EtOH	0.84	13.8	-	[5]
Au-Ag-Pd NWs	1 M KOH +1 M EtOH	0.97	8.6	-	[6]
Au@FePd	1 M KOH +1 M EtOH	0.96	20.2	-	[7]
PdAu/C	1 M KOH +1 M EtOH	1.00	84.2	-	[8]
Ni-W/C	1 M KOH +1 M EtOH	1.60	119.0	-	[9]
Ni-Co/ErN-GO/GCE	1 M KOH +1 M EtOH	1.75	28.5	-	[10]
Ni₃S₄-NiS-rGO	1 M KOH +1 M EtOH	1.35	10.0	-	[11]
Ni/NC	1 M KOH +1 M EtOH	1.17	5.2	-	[12]
Ni-Co/G	1 M KOH +1 M EtOH	1.25	11.5	-	[13]
Ni-S NPs	1 M KOH +1 M EtOH	1.60	45.8	-	[14]

Table S2. Fitting results for EIS spectra over Au/NF electrodes at -0.3V vs. SCE.

Catalyst	Au/NF-0.1	Au/NF-0.4	Au/NF-0.7	Au/NF-1.0	Au/NF-1.3
L₁(H)	1.33E-06	1.41E-06	1.36E-06	1.67E-06	1.56E-06
R₁ ($\Omega \text{ cm}^2$)	13.688	10.632	12.064	12.501	12.6633
R_s ($\Omega \text{ cm}^2$)	2.1284	2.1417	2.1797	2.3494	2.4103
R_{ct1} ($\Omega \text{ cm}^2$)	6.7934	3.7913	2.7864	0.9836	0.19167
CPE₁-T (F)	0.00203	0.00538	0.07408	0.04445	0.00397
CPE₁-P	0.66359	0.56843	0.52122	0.59381	0.94174
R_{ct2} ($\Omega \text{ cm}^2$)	105.26	36.548	20.043	14.057	3.0439
CPE₂-T (F)	9.38E-04	0.00221	0.00538	0.00468	0.00749
CPE₂-P	0.87218	0.82627	0.9603	0.96142	0.88414

Table S3. Fitting results for EIS spectra over Au/NF-1.3 electrode at various potentials.

E/V vs. RHE	0.9 V	1.0 V	1.1 V	1.2 V	1.3 V	1.4 V	1.5 V	1.6 V	1.7 V
L₁ (H)	1.55E-6	1.59E-6	1.69E-6	1.68E-6	1.79E-6	1.80E-6	1.65E-6	1.76E-6	1.82E-6
R₁ (Ω cm²)	11.690	10.655	3.254	3.369	3.706	1.466	1.145	0.793	1.962
R_s (Ω cm²)	2.040	2.049	2.130	2.165	2.378	2.111	2.125	2.098	2.111
R_{ct1} (Ω cm²)	0.719	0.644	0.422	0.203	1.200	0.452	0.257	0.203	0.181
CPE_{1-T} (F)	0.077	0.068	0.014	0.005	0.028	0.180	0.090	0.061	0.022
CPE_{1-P}	0.496	0.520	0.752	0.900	0.766	0.609	0.724	0.765	0.905
R_{ct2} (Ω cm²)	17.206	8.885	3.637	2.516	11.30	1.362	0.274	0.022	0.018
CPE_{2-T} (F)	0.005	0.005	0.005	0.006	0.023	0.094	0.078	0.054	0.008
CPE_{2-P}	0.946	0.961	0.967	0.937	0.964	1.006	1.085	1.675	1.571
L₂ (H)	-	-	-	-	8.859	-	-	-	-
R_L (Ω cm²)	-	-	-	-	2.199	-	-	-	-

Table S4. Fitting results for EIS spectra over NF at various potentials.

E/V vs. RHE	1.3 V	1.4 V	1.5 V	1.6 V	1.7 V
L₁(H)	5.39E-07	8.63E-07	8.05E-07	7.97E-07	9.56E-07
R₁ (Ω cm²)	2.109	3.125	3.182	2.998	2.438
R_s (Ω cm²)	1.010	1.030	1.176	1.007	1.036
R_{ct1} (Ω cm²)	1.419	0.960	0.817	0.757	0.679
CPE₁-T (F)	1.57E-04	8.73E-04	8.18E-04	8.34E-04	6.97E-04
CPE₁-P	0.812	0.889	1.302	0.890	0.892
R_{ct2} (Ω cm²)	28.119	24.812	21.741	12.360	4.409
CPE₂-T (F)	1.95E-03	1.91E-03	4.26E-03	5.72E-03	8.72E-04
CPE₂-P	0.875	0.851	0.747	0.873	0.877

Reference

- [1] L. Bigiani, T. Andreu, C. Maccato, E. Fois, A. Gasparotto, C. Sada, G. Tabacchi, D. Krishnan, J. Verbeeck, J. R. Morante and D. Barreca, *J. Mater. Chem. A*, **2020**, *8*, 16902-16907.
- [2] A. Hatamie, E. Rezvani, A. S. Rasouli and A. Simchi, *Electroanalysis*, **2018**, *31*, 504-511.
- [3] X. Wang, H. Yang, M. Liu, Z. Liu, K. Liu, Z. Mu, Y. Zhang, T. Cheng and C. Gao, *ACS Nano*, **2024**, *18*, 18701-18711.
- [4] M. Zhang, X. Zhang, M. Lv, X. Yue, Z. Zheng and H. Xia, *Small*, **2023**, *19*, 2205781-2205793.
- [5] X. Zhou, Y. Ma, Y. Ge, S. Zhu, Y. Cui, B. Chen, L. Liao, Q. Yun, Z. He, H. Long, L. Li, B. Huang, Q. Luo, L. Zhai, X. Wang, L. Bai, G. Wang, Z. Guan, Y. Chen, C. S. Lee, J. Wang, C. Ling, M. Shao, Z. Fan and H. Zhang, *J. Am. Chem. Soc.*, **2022**, *144*, 547-555.
- [6] S. Zhang, K. Liu, Z. Liu, M. Liu, Z. Zhang, Z. Qiao, L. Ming and C. Gao, *Nano Lett.*, **2021**, *21*, 1074-1082.
- [7] D. Liu, Q. Zeng, H. Liu, C. Hu, D. Chen, L. Xu and J. Yang, *Cell Rep. Phys. Sci.*, **2021**, *2*, 100357-100372.
- [8] W. Zhou, M. Li, L. Zhang and S. H. Chan, *Electrochim. Acta*, **2014**, *123*, 233-239.
- [9] A. Zaher, W. M. A. El Rouby and N. A. M. Barakat, *Fuel*, **2020**, *280*, 118654-118663.
- [10] K. Rahmani and B. Habibi, *RSC Adv.*, **2019**, *9*, 34050-34064.
- [11] S. Azizi, M. B. Askari, M. T. T. Moghadam, M. Seifi and A. Di Bartolomeo, *Nano Futures*, **2023**, *7*, 015002-015015.
- [12] W. Shi, Q. Wang, F. Qin, J. Yu, M. Jia, H. Gao, Y. Zhang, Y. Zhao and G. Li, *Electrochim. Acta*, **2017**, *232*, 332-338.
- [13] Z. Wang, Y. Du, F. Zhang, Z. Zheng, Y. Zhang and C. Wang, *J. Solid State Electrochem.*, **2012**, *17*, 99-107.
- [14] J. Li, X. Tian, X. Wang, T. Zhang, M. C. Spadaro, J. Arbiol, L. Li, Y. Zuo and A. Cabot, *Inorg. Chem.*, **2022**, *61*, 13433-13441.